Dual-feed, single-CCE antenna facilitating inter-band carrier aggregation in LTE-A handsets

Risto Valkonen, Anu Lehtovuori, and Clemens Icheln

Aalto University School of Electrical Engineering, Department of Radio Science and Engineering
P.O. Box 13000, FI-00076 AALTO Email: risto.valkonen@aalto.fi

***Abstract*—A dual-feed single-element antenna based on a capacitive coupling element is proposed as an antenna solution facilitating the use of inter-band carrier aggregation in LTE-Advanced mobile handsets. The antenna operates at the frequency bands 698–960 MHz with the lower frequency antenna feed and at 1710–2690 MHz with the higher frequency feed. No separate radiating elements associated with the two antenna feeds are needed because the signal paths for the different frequencies are isolated by using a novel diplex matching circuit. The general performance of the proposed antenna is good, with total efficiency better than 54 % across the operation frequencies in free space. The isolation between the feeding ports is good, and it does not deteriorate due to the proximity of a user's hand in typical hand grip situations.**

***Index Terms*—mobile antennas, impedance matching, diplexers, LTE communication systems**

I. Introduction

To support increased data rates in future mobile communication systems, carrier aggregation (CA) technology is introduced in Long Term Evolution - Advanced (LTE-A) specifications by the 3rd Generation Partnership Project (3GPP) [1]. Aggregating two or more component carriers (CC) allows increased simultaneous transmission bandwidth, and consequently, improved data throughput [2]. The carrier aggregation may be implemented as intra-band CA or as inter-band CA. In the intra-band carrier aggregation, the component carriers are within the same operating band, forming either a continuous aggregated bandwidth or a set of closely spaced non-contiguous sub-bands. Inter-band CA involves aggregation of carriers in different operating bands.

From the antenna point of view, the main prerequisite for CA is simultaneous impedance matching at each frequency band of the used CA configuration. This should not be a major challenge, since many contemporary multi-band antennas in mobile handsets readily fulfill the typical impedance matching requirements of almost all of the CA bands simultaneously. By contrast, the challenge of inter-band CA is more demanding for the transceiver RF front-end.

In a conventional RF front-end architecture for mobile handsets, there is a single feed for cellular antennas. Most handset antennas are designed by assuming this single-feed RF front-end interface, e.g. [3]. When using the conventional approach, the inter-band CA would be enabled only if the duplexers of the operation bands used for CA were connected to the antenna feed simultaneously. This means practically that the duplexers of these different frequency bands should be matched together [4], which is an insurmountable task to implement for all of the CA band pairs in a mobile handset for global operation.

Fortunately, the duplexer matching problem can be relieved by antenna design. It is sufficient to design an antenna with multiple feeding points such that each antenna feed operates at a dedicated frequency band and is isolated from all other feeds at this band. The interface from the antenna to the RF front-end will then have naturally isolated paths for the signals at different frequency bands, and the matching of the duplexers is not an issue.

The antenna solution proposed in this paper is a dual-feed antenna based on a single capacitive coupling element (CCE) and a novel diplex matching circuit. There is one antenna feed for lower LTE-A frequencies and another for higher LTE-A frequencies. This dual-feed solution solves the duplexer matching problem in most of the cases. The use of single CCE enables the use of the entire antenna volume all the time, which is important at the lowest frequencies of operation. Given the fundamental limitations of small antennas, the low frequencies are the most critical from the efficiency and bandwidth points of view. The ability to use the antenna volume optimally results in more efficient radiation compared to a structure having the antenna volume divided between different frequencies.

II. LTE-A inter-band carrier aggregation

In the release 10 (R10) of the 3GPP specifications [1], the carrier aggregation is allowed only between 3GPP operating bands 1 and 5 at 2.1 GHz and 850 MHz. In the next, currently incomplete 3GPP release 11 (R11), there are twelve different pairs of operating bands defined for inter-band CA according to the current plan, see Table I [5].

Ten of the 12 CA band pairs for 3GPP R11 are such that one of the frequency bands is below 1 GHz and the other is above 1.7 GHz. Thereby, using a dual-feed antenna with one feed for frequencies below 1 GHz and one for higher frequencies, the majority of the CA band pairs could be realized without need of the demanding duplexer matching. This idea is exploited in the antenna presented in this paper.

Out of the remaining two frequency pairs, the first one involves bands 1 and 21 at 2.1 GHz and 1.4 GHz, respectively. Since the use of band 21 is geographically very limited (mainly

978-88-907018-3-2/13

to Japan), this CA band pair is unlikely to be implemented in mobile handsets intended for global operation. The second remaining pair involves bands 3 and 7 at 1.8 GHz and 2.6 GHz, respectively. Both of these bands are used widely, so this CA band pair will be discussed later in Section V.

TABLE I
INTER-BAND CA PAIRINGS IN 3GPP TS36.101 V11.2.0 [5]

Band no.	Downlink (MHz)	Uplink (MHz)	Band pair(s) no.
1	1920–1980	2110–2170	5,18,19,21
2	1850–1910	1930–1990	17
3	1710–1785	1805–1880	5,7,20
4	1710–1755	2110–2155	12,13,17
5	824–849	869–894	1,3
7	2500–2570	2620–2690	3,20
12	699–716	729–746	4
13	777–787	746–756	4
17	704–716	734–746	2,4
18	815–830	860–875	1
19	830–845	875–890	1
20	832–862	791–821	4,7
21	1447.9–1462.9	1495.9–1510.9	1

III. MULTI-FEED ANTENNAS IN MOBILE HANDSETS

Handset antennas with multiple feeds include e.g. the antennas for MIMO (Multiple input, multiple output) and other diversity systems, where distinct antenna elements operate simultaneously at the same frequency band. However, in this paper the focus is not on antenna diversity, but on carrier aggregation. Thereby, the concept of dual-feed (multi-feed) antennas is discussed from another point of view than usually.

Dual-feed antennas with independent feeds for lower and higher frequencies have been designed e.g. in [6], [7], and even a triple-feed design has been presented as an enabler of the inter-band CA [4]. Common to these designs is that the separate feeds are assigned for different antenna elements. However, distributing the antenna volume to multiple parts may lead to impaired antenna performance at the lowest frequencies of operation, at which the antenna performance would benefit from the maximum available antenna size. One of the main targets in designing the antenna proposed in this paper was to implement one CCE operating at all desired frequencies and capable of inter-band CA.

A. Dual-feed single-element antenna

Electromagnetic simulations (IE3D) and circuit simulations (AWR Design Environment) were used in the design of the dual-feed antenna. The proposed CCE antenna geometry is presented in Fig. 1. The design is based on a very similar single-feed CCE antenna presented in [8]. As it can be seen in the drawing, the CCE itself is a very simple rectangular element without fine details. The element is an off-ground CCE occupying a total volume of $10 \times 50 \times 5$ mm^3 including the ground clearance. The 100×50 mm^2 ground plane consists of the metallic chassis of the mobile handset.

The speciality of this antenna is that the CCE is fed through two feeding strips. The narrow rectangular feeding strip is located along the long axis of the chassis, and the trapezoidal shape feeding strip is located 6 mm offset from that axis (see Fig. 1). The purpose is to feed the CCE from two independent feeding ports such that the feeds operate at different frequencies and are well isolated from each other. This can be implemented with a matching circuitry.

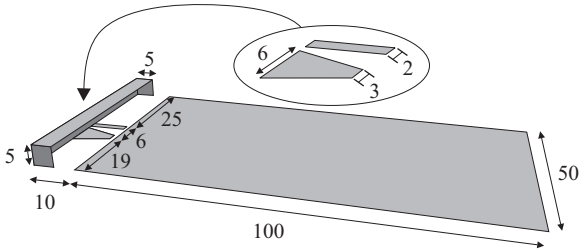

Fig. 1. Geometry of the metallic parts of the proposed dual-feed antenna. Dimensions in millimeters.

The rectangular feeding strip located along the long axis of the chassis is intended for frequencies 700–960 MHz. The narrow and inductive feeding strip suits the low frequency operation, compensating partly the inherently capacitive impedance of the CCE at low frequencies. The feeding strip located offset from the long axis of the chassis is meant for 1710–2690 MHz frequencies. The trapezoidal shape minimizes excess series inductance and parallel capacitance caused by the feeding strip at the high frequencies where the inherent impedance of the CCE is on the inductive side. The placement of the trapezoidal feeding strip has been designed so that a natural resonance of the CCE is excited at about 2.7 GHz [8]. This resonance helps in reaching enough bandwidth at the high frequencies of operation.

In addition to the feeding strips, also additional reactive impedance matching components are needed to realize the desired antenna operation at the target frequencies. This is discussed next.

B. Matching circuit as diplexer

Matching circuits are typically needed with capacitive coupling element antennas because the CCE alone is often poorly matched at the desired frequencies of operation [9]. In the case of the dual-feed CCE, it is not sufficient to just match each feeding port of the antenna at their respective operation frequencies, but the ports need to be isolated as well. Without any filtering, the inherent isolation between the ports is poor, especially at low frequencies, because the feeding points at the CCE side are close to each other and galvanically connected. Thereby, the matching circuits will have to implement the functionality of a diplexer.

The diplex matching circuit for the antenna of Fig. 1 was designed based on a few very basic rules: The circuit branch for the lower frequencies should implement a low-pass response and the circuit branch for the higher frequencies should have a high-pass response. In addition, the output ports should see each other as a high reactive impedance at their respective operation frequencies. Also the information of the

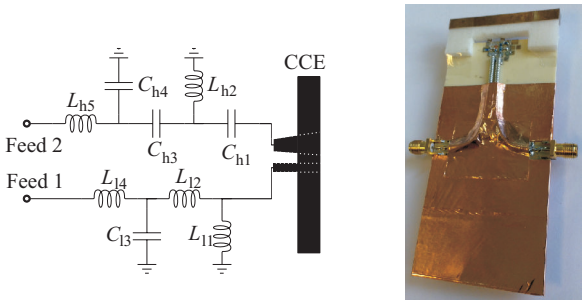

Fig. 2. Proposed diplexing matching circuit (left) and dual-feed CCE antenna prototype (right). The copper tape shielding on the front side of the prototype was used to eliminate a spurious resonance caused by the two feeding coaxial cables.

CCE impedance was utilized. At low frequencies, the CCE is highly capacitive and should be matched with a dominantly inductive circuit. At higher frequencies, the inherently inductive input impedance of the CCE is compensated with a capacitive circuit.

The optimization lead finally to the design shown as a schematic in Fig. 2. The component values of the matching circuit are listed in Table II. The matching impedance was 50 Ω. As a general note, the usual multiplexer synthesis methods, e.g. [10], [11], could not be used in this case. The common port junction, which is within the CCE, is very complex to model over the required wide frequency range.

TABLE II
MATCHING CIRCUIT COMPONENTS OF THE DUAL-FEED CCE (FIG. 2).

L_{l1} (nH)	L_{l2} (nH)	C_{l3} (pF)	L_{l4} (nH)	C_{h1} (pF)	L_{h2} (nH)	C_{h3} (pF)	C_{h4} (pF)	L_{h5} (nH)
10	18	2.4	15	0.5	4.7	0.5	0.1	1.5

IV. ANTENNA PERFORMANCE

A. Free space performance

The antenna prototype (Fig. 2) was manufactured on a Rogers 4003C PCB substrate using inductors from Murata's series LQW18 and capacitors from series GQM18 as the matching components. The exception was the component C_{h4} (0.1 pF), which was implemented directly on PCB. The CCE was made from 0.15 mm thick sheet of copper.

The simulated and measured impedance matching results of the antenna are presented in Fig. 3. The lower frequency feed for the antenna (port 1) is matched at the low-band LTE-A frequencies (698–960 MHz), and the higher frequency feed (port 2) is matched at the high-band LTE-A frequencies (1710–2690 MHz) with better than 6 dB return loss. The simulation and measurement results agree relatively well.

The measured total efficiency (η_{tot}) of the antenna is shown in Fig. 4. Total efficiency at the LTE-A frequencies is 54 – 91 %, which indicates a good performance for a mobile handset antenna. Radiation efficiency (η_{rad}) remains above 60 %.

The isolation between the two antenna feeds is presented in Fig. 5. Better than 20 dB isolation is achieved between

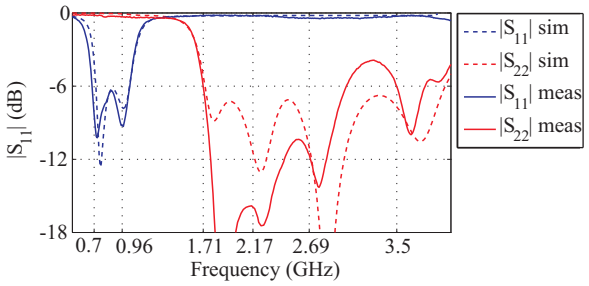

Fig. 3. Simulated and measured impedance matching of the dual-feed CCE antenna.

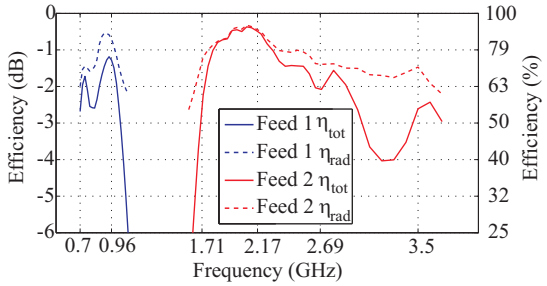

Fig. 4. Measured total and radiation efficiency of the dual-feed CCE antenna.

the ports. Additional filters between the feeding port and the matching circuit could still improve the isolation significantly. However, the isolation between the ports is readily enough to implement CA between a low-band frequency and a high-band frequency without need for built-in matching of the corresponding duplexers. Furthermore, the isolation values are about the same as with the designs implemented with separate antenna elements [4], [7]. In [6], the isolation was not reported.

B. User hand effects

Mobile handset antennas need to operate not only in free space, but also in the immediate vicinity of the mobile phone user. Therefore we measured the antenna prototype also with SPEAG's SHO V2RB and SHO V2RD hand phantoms in several positions. The two grips which lead to the worst total efficiency results are shown in the photographs in Fig. 6. The grip on the left is a typical 'talking grip' with the index finger partly covering the antenna element, which is located at the top of the handset. During the measurements, the antenna was inside an enclosure made of polycarbonate. The thickness

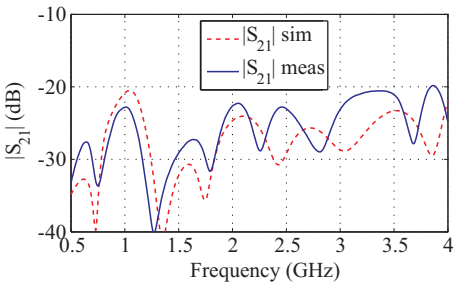

Fig. 5. Simulated and measured isolation of the CCE antenna feeding ports.

Fig. 6. Left: The dual-feed antenna with SHO V2RB 'talking grip' hand phantom. Right: The antenna with SHO V2RB 'browsing grip' hand phantom. The location of the CCE in each case is highlighted.

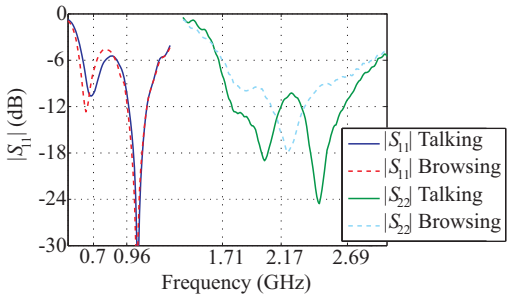

Fig. 7. Measured impedance matching of the antenna with the hand grips shown in Fig. 6.

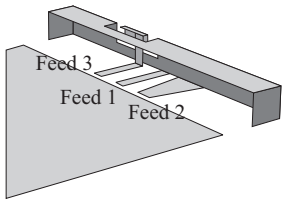

Fig. 8. Possible implementation of an additional 2.6 GHz diversity antenna without increasing antenna volume.

of the enclosure is 1 mm, which constitutes the minimum distance between the CCE and the index finger. The grip on the right is a 'browsing grip' with the CCE located at the bottom part of the handset. Now the thenar muscles and the ring finger are the hand parts closest to the CCE.

The measured impedance matching result of the antenna with the two hand grips is shown in Fig. 7. It can be seen that the matching result is not significantly deteriorated due to the hands. This was also expected based on the results of [12]. Isolation between the ports remained almost unchanged compared to the free space case, thereby not affecting the antenna performance in the CA mode.

On the other hand, the total and radiation efficiencies of the antenna were decreased. Table III shows the change of η_{tot} and η_{rad} of the antenna resulting from the additional losses due to the hand grips. The talking grip decreases the total efficiency of the antenna by 3.5–5 dB, and the browsing grip causes up to 7.8 dB decrease of total efficiency. These losses are about 1 dB higher than those reported in [12] for the 5 mm thicker antenna structure. The antenna prototype of this paper together with the polycarbonate enclosure is only 7 mm thick (compared to 12 mm in [12]), and consequently the average distance between the chassis and the hand tissue is smaller, causing stronger absorption by the hand. Assigning additional space between the antenna and the enclosure would help in decreasing the absorption losses.

The specific absorption rate (SAR) of the geometrically almost identical antenna in [8] has been studied and the antenna was found to satisfy the ICNIRP guidelines for exposure to electromagnetic fields, [8].

TABLE III
MEASURED CHANGE OF TOTAL AND RADIATION EFFICIENCY OF THE ANTENNA (DB) DUE TO THE HAND GRIPS, COMPARED TO FREE SPACE

		750 MHz	900 MHz	1800 MHz	2100 MHz	2500 MHz
talking	$\Delta\eta_{\mathrm{tot}}$ (dB)	-5.0	-4.9	-3.8	-4.0	-3.6
	$\Delta\eta_{\mathrm{rad}}$ (dB)	-5.1	-4.8	-3.7	-4.0	-3.6
browsing	$\Delta\eta_{\mathrm{tot}}$ (dB)	-6.4	-6.5	-7.2	-6.6	-7.8
	$\Delta\eta_{\mathrm{rad}}$ (dB)	-5.8	-6.5	-6.7	-6.5	-7.2

V. ANTENNA DIVERSITY CONSIDERATIONS

Based on the presented results, the dual-feed CCE antenna is able to handle 10 of the 12 frequency pairs associated with inter-band CA. The eleventh band pair with global importance (bands 3 and 7) could be implemented by matching the corresponding duplexers. Since this has to be made with one pair of duplexers only, it would unlikely be an impossible task.

A. CA for bands 3 and 7

Another option for implementing the CA between bands 3 and 7 is to involve a dedicated diversity antenna for 2.6 GHz. The antenna element can be made very small and it can be implemented within the same antenna volume as the main antenna e.g. by making the main element hollow and placing the diversity antenna inside the main antenna's volume as in [13]. An example of this kind of configuration is seen in Fig. 8 where the dual-feed CCE presented in this paper is modified to include a small diversity element associated with a third feeding port.

The antenna geometry of Fig. 8 was simulated as perfect electric conductor (PEC), and combined with a matching circuit consisting of 14 lumped reactances. The simulated impedance matching of this example structure is shown in Fig. 9, and the isolation between the ports is shown in Fig. 10. The results indicate that the small element would operate well at the LTE-A band 7. The isolation between the ports 2 and 3 at the bands 3 and 7 is close to 20 dB, being well sufficient for the inter-band CA. As a bonus, the small diversity element could be used also for MIMO at 2.6 GHz.

B. MIMO challenges

In addition to carrier aggregation, LTE-A includes also the MIMO option for enhanced data rates. The use of MIMO

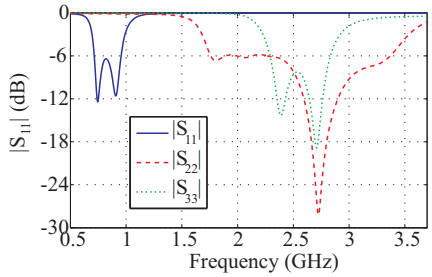

Fig. 9. Simulated example showing the impedance matching of the triple-feed antenna in Fig. 8. There is a matching circuit consisting of 4–5 lumped reactances at each port.

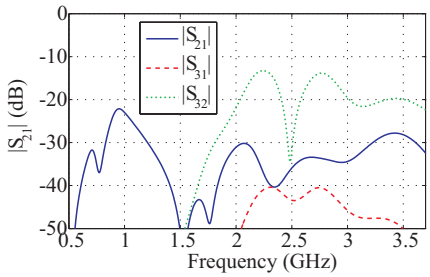

Fig. 10. Simulated example showing the isolation between the ports of the triple-feed antenna in Fig. 8.

requires at least two antenna elements operating at the same frequency band. In the case of the 2.6 GHz band, the diversity element could be implemented within the same volume as the main element. However, if MIMO operation at lower frequencies is desired, it would be wiser to designate additional volume for the diversity antenna.

Considering the simultaneous use of MIMO and inter-band CA, it doesn't seem wise to first make separate antenna elements for low and high frequencies to implement CA, and then add the corresponding diversity elements for MIMO operation. This work, having shown that the CA can be implemented also with a single antenna element, can serve as a basis for implementing CA and MIMO simultaneously in a multi-antenna handset. One possible implementation for coexistent MIMO and CA is to use a multi-feed main antenna element like the one presented in this paper, and for example a balanced antenna located at the opposite end of the chassis like in [14] as the diversity element. The benefit of a balanced antenna is good isolation with the (main) chassis antenna, but on the other hand, the instantaneous bandwidth of the balanced antenna would be narrow [14]. In that case, the diversity element should be made tunable.

VI. Conclusion

A single-element CCE antenna with two antenna feeds was designed and manufactured. The antenna facilitates inter-band carrier aggregation in LTE-A mobile systems by relieving the RF front-end duplexer design. Compared to the previous dual-feed or multi-feed antenna solutions, the single-CCE approach utilizes the antenna volume more efficiently for optimal radiation performance also at the lowest frequencies of operation, since the entire antenna volume is available at all frequencies.

Also the general performance of the antenna is competitive in comparison to other multi-standard handset antennas. The antenna operates at the LTE-A system frequencies 698–960 and 1710–2690 MHz with good impedance matching level and efficiency. The performance of the antenna in the proximity of a user's hand was measured and the results were as desired. The antenna operates near the user's body similarly as the comparable single feed CCE antennas. The isolation between the feeding ports of the antenna remains good across the used frequency range, regardless of the antenna being in free space or being held in hand.

To support the MIMO option of LTE-A systems, the antenna presented in this paper would require the implementation of a diversity element. This is an important topic for future research, which benefits from the results of this work.

References

[1] 3GPP Technical Specification 36.101, "E-UTRA User Equipment (UE) radio transmission and reception (Release 10)," V10.8.0, Sept. 2012.

[2] G. Yuan, X. Zhang, W. Wang, and Y. Yang, "Carrier aggregation for LTE-advanced mobile communication systems," *IEEE Commun. Mag.*, vol. 48, no. 2, pp. 88–93, 2010.

[3] Z. Ying, "Antennas in cellular phones for mobile communications," *Proc. IEEE*, vol. 100, no. 7, pp. 2286–2296, 2012.

[4] P. Ikonen, J. Ellä, E. Schmidhammer, P. Tikka, P. Ramachandran, and P. Annamaa, "Multi-feed RF front-ends and cellular antennas for next generation smartphones," Pulse Electronics Corporation, Technical article, 2011, (Cited 16 Oct. 2012). [Online]. Available: http://www.pulseelectronics.com/download/3755/indie_technical_article

[5] 3GPP Technical Specification 36.101, "E-UTRA User Equipment (UE) radio transmission and reception (Release 11)," V11.2.0, Sept. 2012.

[6] K. R. Boyle, Z. Liu, T. Huang, Y. Sun, A. Simin, E. Spits, O. Kuijken, and T. Roedle, "A multi-band, dual-antenna and antenna interface module system for mobile phones," in *Proc. Int. Workshop Antenna Technology: Small and Smart Antennas Metamaterials and Applications IWAT '07*, 2007, pp. 53–56.

[7] P. Bahramzy and M. Sager, "Dual-feed ultra-compact reconfigurable handset antenna for penta-band operation," in *Proc. IEEE Antennas and Propagation Society Int. Symp. (APSURSI)*, 2010.

[8] R. Valkonen, J. Ilvonen, C. Icheln, and P. Vainikainen, "Inherently non-resonant multi-band mobile terminal antenna," *Electronics Letters*, vol. 49, no. 1, pp. 11–13, Jan. 2013.

[9] J. Villanen, J. Ollikainen, O. Kivekäs, and P. Vainikainen, "Coupling element based mobile terminal antenna structures," *IEEE Trans. Antennas Propag.*, vol. 54, no. 7, pp. 2142–2153, Jul. 2006.

[10] R. Cameron and M. Yu, "Design of manifold-coupled multiplexers," *Microwave Magazine, IEEE*, vol. 8, no. 5, pp. 46 –59, Oct. 2007.

[11] G. Macchiarella, "Synthesis of star-junction multiplexers," *Microwave Magazine, IEEE*, vol. 12, no. 6, pp. 101 –109, Oct. 2011.

[12] R. Valkonen, J. Ilvonen, and P. Vainikainen, "Naturally non-selective handset antennas with good robustness against impedance mistuning," in *Proc. 6th European Conf. Antennas and Propagation (EuCAP)*, 2012, pp. 796–800.

[13] A. Cihangir, F. Sonnerat, F. Ferrero, C. Luxey, R. Pilard, F. Gianesello, and G. Jacquemod, "Design of traditional and a novel space-efficient antenna-coupling elements for lower LTE/GSM mobile phones," in *Loughborough Antennas and Propagation Conference (LAPC)*, Nov. 2012.

[14] J. Ilvonen, O. Kivekäs, A. A. H. Azremi, R. Valkonen, J. Holopainen, and P. Vainikainen, "Isolation improvement method for mobile terminal antennas at lower UHF band," in *Proc. 5th European Conf. Antennas and Propagation (EuCAP)*, 2011, pp. 1238–1242.